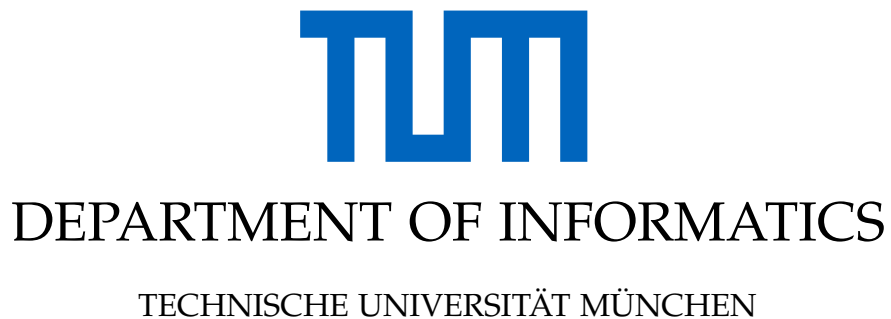


Master's Thesis in Informatics: Robotics, Artificial Intelligence and
embeded system

Retinal surgery simulation system based on SOFA

Jingsong Liu





Master's Thesis in Informatics: Robotics, Artificial Intelligence and
embeded system

Retinal surgery simulation system based on SOFA

Author: Jingsong Liu
Supervisor: Dr. Mingchuan Zhou
Advisor: Prof. Knoll
Submission Date: 30.06.2022



I confirm that this master's thesis in informatics: robotics, artificial intelligence and embeded system is my own work and I have documented all sources and material used.

Munich, 30.06.2022

Jingsong Liu

Abstract

Nowadays there are more than hundred million patients were identified as having retinal diseases. However, because of the high degree of difficulty in retinal surgery, often ophthalmologists need long surgical training to qualify for surgery. With this motivation, we developed the first retinal vascular injection surgery simulation system. Based on SOFA and its separate model principle, the simulation system which contains both needle and eye models can not only have realistic visualization but also can reach real-time control (more than 30 *fps/s*). Two types of input controller are supported (keyboard and SpaceMouse). Six experimenters were invited to participate in the experiment in order to obtain a learning curve and a comparison of the efficiency of the two input methods.

Besides, based on the Finite-Element-Method simulation system, the relationship between insertion angle of the micro-needle and puncture force was investigated. Experiments show that within a certain range, the larger the insertion angle, the smaller the puncture force required to puncture the vessel. Finally a theoretical mechanical model is given to explain such relationship.

Through the development of the simulation system and the study of the needle insertion angle, we hope that our efforts will enable ophthalmologists to understand the process of retinal surgery and improve the proficiency and confidence of ophthalmologists and therefore increase the success rate of real-world retinal disease operations.

Contents

Abstract	iii
1 Introduction	1
1.1 Retinal disease surgery	1
1.2 Robot-assisted retinal surgery	1
1.3 Surgical Simulation System	2
1.4 Contributions	3
2 State of the Art	5
2.1 Robot-assisted Retinal Surgery	5
2.2 Retinal Surgical Simulation System	8
2.3 Needle-puncture force detection	9
3 SOFA based puncture force detection	10
3.1 Introduction to SOFA framework	10
3.2 Constraint forces solver in SOFA	10
3.3 SOFA models related to puncture experiments	11
3.3.1 Visual models	11
3.3.2 Collision models	14
3.3.3 Force models	14
3.4 SOFA based puncture experiments	15
3.5 Conclusion	18
3.6 An mechanics-based explanation	20
3.7 Validation and Discussion	21
4 SOFA based retinal surgery simulation system	23
4.1 Models	23
4.1.1 Eyeball	23
4.1.2 Retinal Vessel	23
4.2 Transformation	23
4.3 Controller	25
4.3.1 Keyboard	27
4.3.2 SpaceMouse	27
4.4 Trauma detection	27
4.5 Graphic view	29
4.6 Experiment	29
4.6.1 Task description	29

Contents

4.6.2	Evaluation system	30
4.6.3	Experiment settings	30
4.6.4	Experiment results	31
4.6.5	Experiment conclusion	31
5	Limitations	33
6	Conclusion	34
List of Figures		35
Bibliography		37

1 Introduction

Nowadays there are more than hundred million patients were identified as having retinal diseases.

1.1 Retinal disease surgery

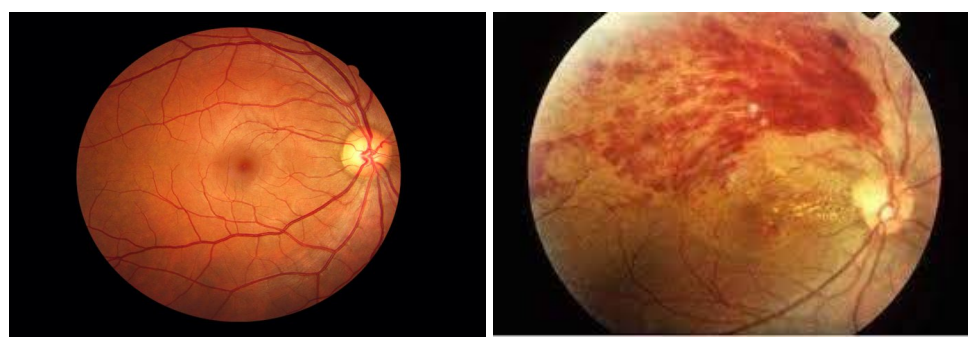
But due to limitations in the human capabilities, retinal microsurgery is one of the most challenging surgical tasks. The challenges include the need for highly precise movements in a very small and fragile environment, which is also difficult to access. It is further hindered by poor visibility, movements of the patient and hand tremor of the surgeon. Retinal surgery needs critical surgical skills and considerations. In 2019, there have been more than 342 million patients having retinal disease, mainly with age-related macular degeneration(196 million) and diabetic retinopathy(146 million) [19].

Due to the high degree of difficulty and risk that distinguishes retinal surgery from ordinary surgery, two methods are expected to improve the success of the operations: robot-assisted retinal surgery and medical simulation teaching systems.

1.2 Robot-assisted retinal surgery

Robot-assisted surgery is considered as the solution for reducing the work intensity and operation difficult, as well increasing the surgical outcomes in retinal surgery.

In 2021 Dishi Medical Technology Co. were found to develop a high-precision surgery robots for retinal surgery operations. The newly developed robots can achieve 5 um precision



(a) Normal retinal

(b) Retinal vein occlusion

Figure 1.1: Normal human retinal and retinal vein occlusion

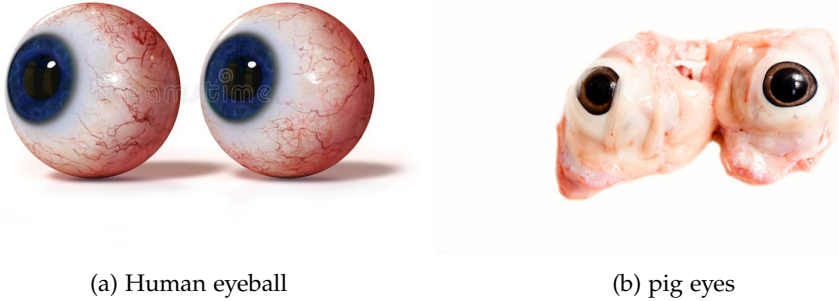


Figure 1.2: Pig eyes v.s. human eyes

in four degrees of freedom, three rotation and one translation, included(??). Needles and forceps are adapted at the end part of the robot, which are corresponding to retinal vascular injection treatment and retinal peeling treatment, respectively. The indications are retinal vein occlusion and retinal detachment. The successful application of robotics holds the promise of greatly reducing the difficulty of surgery, increasing surgeons' confidence and ultimately contributing to the success rate of surgery.

1.3 Surgical Simulation System

Because of the high degree of difficulty in retinal surgery, often ophthalmologists need long surgical training to qualify for surgery. For example, ophthalmology residency programs in Germany usually take 5 years. The high cost of operating room space coupled with decreasing reimbursements have further limited operating room-based training [12]. Additionally, Ophthalmic surgery, especially retinal surgery, requires a large number of eye biopsies for experimentation. Often hospitals choose porcine eyeballs for experiments because they are essentially the same size and structure as human eyes, with corneal refraction and corneal thickness more similar to human eyes than dogs and rabbits [16]. Usually the pig eye is only valid for 12 hours after removal from the living body, longer than that the eye will become cloudy. The surgeon has to complete retinal puncture and debridement training during this time. Often the eyes are brought back from the slaughterhouse freshly removed from the living body, and there is a risk of contaminating the surgical training room with residual blood and bacteria, and microscopically, the health of the doctor is at risk from various sources of disease in the slaughterhouse.

Thus, under such pressures from time cost, training supplies cost and health and safety in the operating room, there has been an increasing use of simulators in modern retinal surgical training.

A simulator is usually a device or model used for training individuals by imitating situations they will encounter in real life[11]. Working with simulators provides the trainee lots of opportunities to practice techniques and get familiar with the process complication until

they could qualified perform based on the evaluation system in the simulated operation. Importantly, surgical simulation promotes repeated practice in a setting that forgives failure, and thus provides the opportunity to learn from one's errors without causing major harm. The implication is that repetitive use of surgical simulations will reduce operative times, lower complication rates and improve patient outcomes[4].

1.4 Contributions

Based on the SOFA simulation framework, the contributions of this work focus on the following.

- Design and develop a simulation system specifically for retinal surgery. To the our best of knowledge, this is the first simulation system designed specifically for retinal surgery in the world. The surgical system is compatible with two input methods: keyboard and SpaceMouse joystick[1]. The keyboard is easier and more familiar to operate. while SpaceMouse as joystick is more intuitive and convenient for the user to form a mapping relationship between controlling and movements of needle. The system is also designed to simulate retinal injection surgery with appropriate difficulty and content similar to that of real-world retinal surgery. Also as feedback, an evaluation system based on time and number of traumas is equipped.
- Experiments were designed to obtain the learning curve of the simulation system. A total of 6 people participated in this experiment. Each participant crossed the keyboard and SpaceMouse handle to record the time and number of traumas to complete the experiment. The aim is to compare the learning curve of each participant with the same input method and conclude the controlling efficiency via comparison of two different input methods.
- Also based on the Finite-Element-Method simulation system, the effect of different insertion angles on the insertion force when the needle is inserted into the vessel was investigated. In which three different mesh models are chosen and compared, the one that best fits the real situation is selected, and the angle of needle insertion into the vessel is variant to study relationship between insertion angle and puncture force. Finally a theoretical model is also given to explain the puncture force change.

In view of the high difficulty and risk of retinal surgery, we hope to improve the success rate of real-world retinal surgery for patients with retinal diseases by studying the insertion angle of fine needles and developing a surgical simulation system.



Figure 1.3: SpaceMouse: 6 DOFs joystick

2 State of the Art

During the implementation of the simulation surgical system, several tasks in many fields are included. This section will present some previous works in these directions related to this thesis.

2.1 Robot-assisted Retinal Surgery

The first robotic system developed for intraocular procedures was reported in 1989[2]. Since then, a large number of retinal surgical systems were developed. The Micron from Johns Hopkins University[9], was designed as a handheld actively stabilized tool to increase accuracy in microsurgery. In retinal surgery, it is able to remove involuntary motion, such as tremor, by the actuation of the tip to counteract the effect of the undesired handle motion. Technical University of Munich has also invented RAMS[10], a hybrid parallel-serial robot comprising of prismatic piezo actuators. It is developed for microscale motions and is stable in the presence of vibrations common in operation room (OR). The robot was designed for a hospital scenario, and even designed an assembly device to fit into a hospital bed.

The first clinical successes on human patients was achieved by the Preceyes Surgical System in 2018[18]. In this study, 12 patients requiring dissection of the epiretinal or inner limiting membrane over the macula were randomly assigned to either undergo robot-assisted-surgery or manual surgery, under general anaesthesia. Surgical results with robotic assistance were equally successful compared to those without, albeit longer with use of the robotic system. In addition, the Preceyes robot was used to demonstrate injection of recombinant tissue plasminogen activator into the subretinal space, further demonstrating the degree of achievable precision.

For now Preceyes Surgical System is the only commercially available product. It provides surgeons with a precision better than $20 \mu\text{m}$ to position and hold instruments. The Preceyes team are keeping innovating and researching in OCT field and for now at least 3 products are currently utilized for surgical and research purpose in Europe.

University of Leuven, Belgium did another clinical experiment on human-patients with their own-invented robotic system. The research group used the co-manipulated robotic system to perform retinal vein cannulation(RVC) operation on 4 patients. The results show that it is technically feasible to safely inject an anticoagulant into a retinal vein of an RVO patient for a period of 10 min with the aid of the presented robotic technology and instrumentation.

Overall, the worldwide rollout of robotic assistance in retinal surgery will take longer and more comprehensive reliability validation.

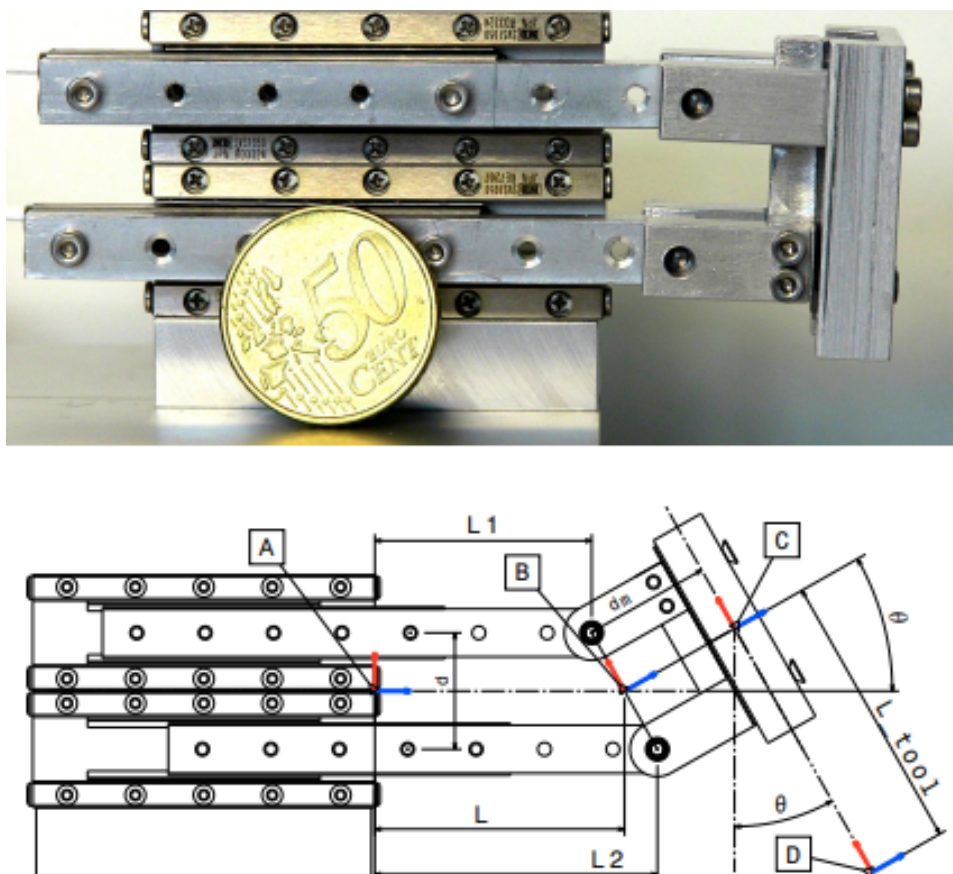


Figure 2.1: Parallel Coupled Joint Mechanism (PCJM) used in TUM-invented robots RAMS

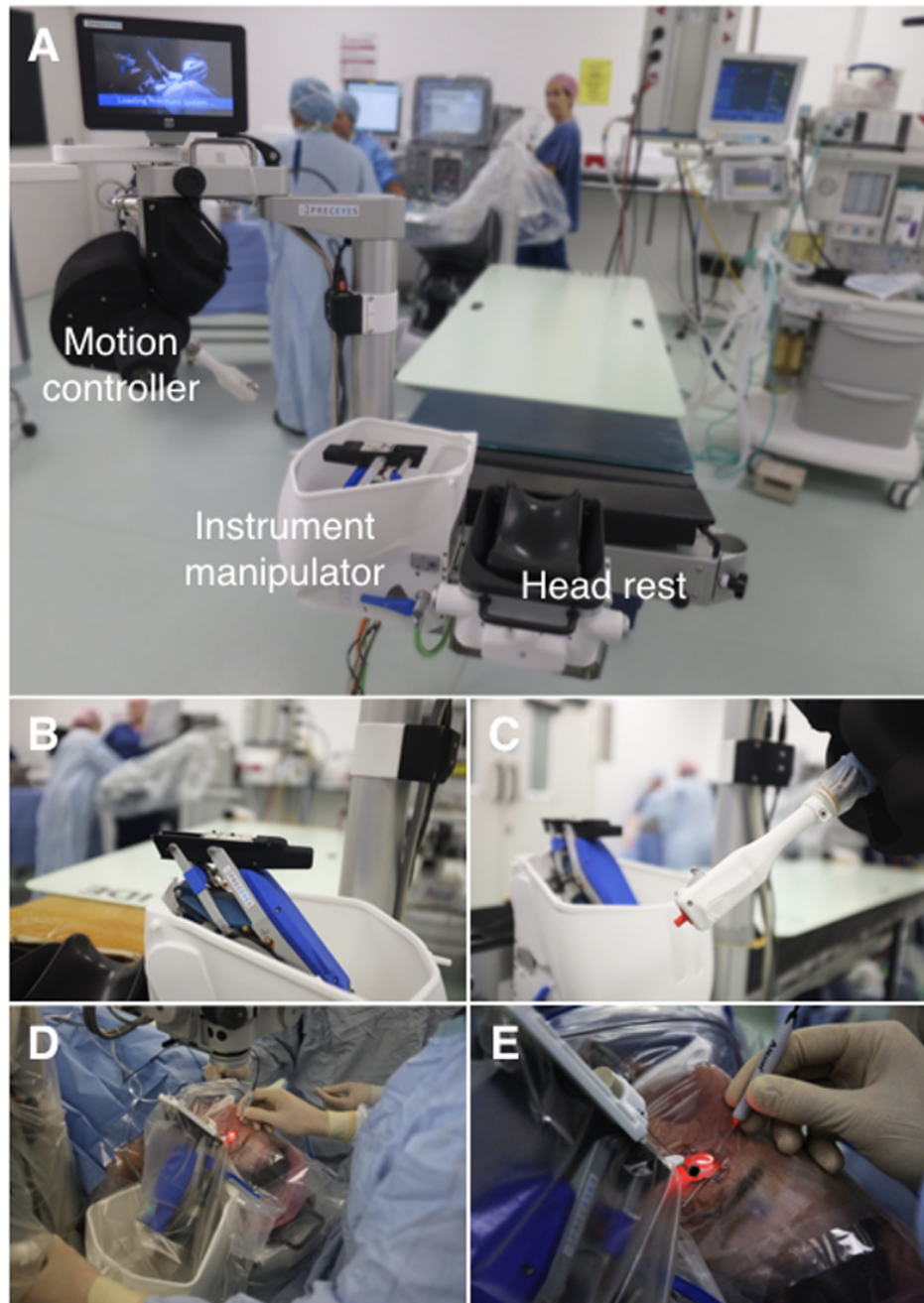
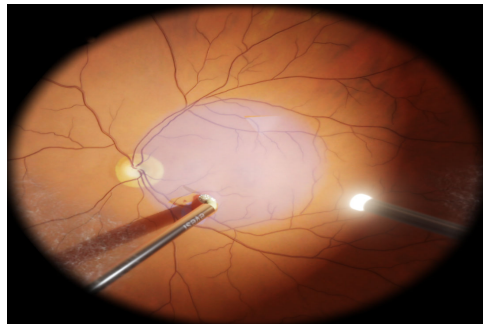


Figure 2.2: First-In-Human Robot-Assisted Subretinal Drug Delivery with Preceyes Robots



(a) Eyesi Simulator



(b) Membranes removal module

Figure 2.3: Eyesi Simulator and retinal surgery training modules

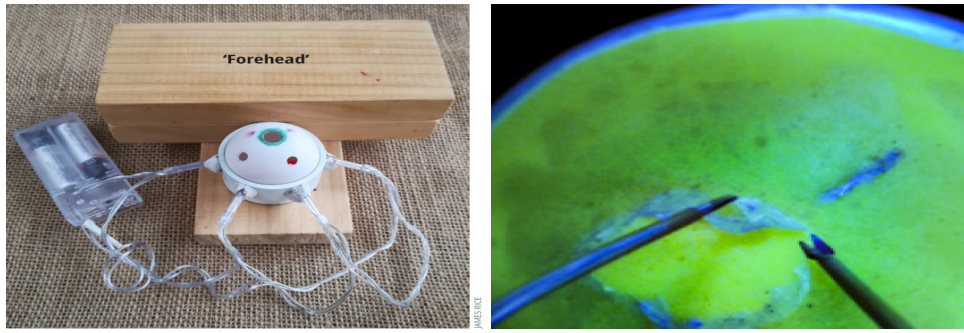
2.2 Retinal Surgical Simulation System

Because of the lack of the usage of robot assistance in retinal surgery, ophthalmologists mostly perform the retinal surgery by themselves. So usually they need long surgical training due to the high degree of difficulty. To this degree simulation system is a good choice considering the costs.

Eyesi Surgical[15], developed by Haag-Streit Simulation (Mannheim, Germany), is a virtual reality simulator for intraocular surgery training. The Eyesi platform can be equipped with interfaces for cataract and vitreoretinal surgery. Besides it provides step-by-step training tutorial from beginners to experts, and also an independent and complete evaluation system, allowing the trainers to systematically improve their skills. In retinal training model there are the removal of epiretinal membranes, or the treatment of retinal detachments with oil or gas endotamponades available. On a technical level, Eyesi surgical simulation system contains a human head model and a human eye prosthesis. The display shows the microscope screen. Depending on the training task, the lens or retina can interact and deform with the simulation apparatus. The highly realistic simulation of interaction with tissue in real-time increases trainees' surgical experience – without risk for real patients.

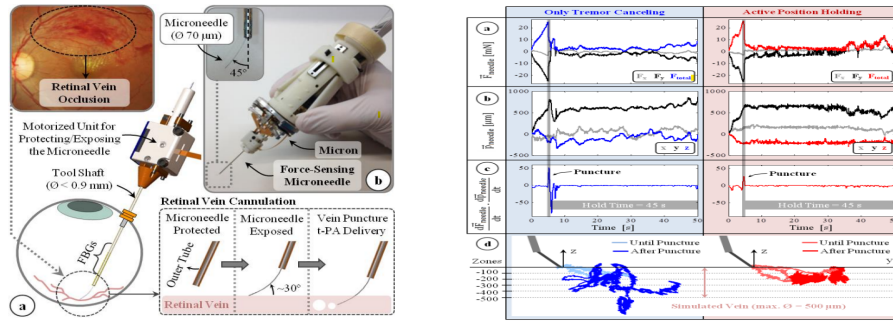
In addition to high-end commercial products like eyesi, some researchers have invented some very low-cost alternatives to the eyeball. James Rice made a low-cost eyeball model in 2019[13] that costs less than \$20 using ping pong balls, liquid glue and Spray-on membrane dressing. The model is simple to make and can be trained for the procedure of retinal detachment, making it suitable for training use in clinics in third-world countries.

And as far as targeting retinal vascular injection procedures, no simulation system has been developed for a similar task to the authors' knowledge. This master's thesis also aims to fill a gap in this field and could help to improve the skills of ophthalmologists performing RVC surgery.



(a) James's Complete low-cost eyeball model (b) Manipulation of a fine membrane

Figure 2.4: A low-cost complete eyeball for retinal surgery[13]



(a) The needle is bent 45° to approach the vein at 30° . (b) Force measurement during the insertion of needle towards vinyl layer.

Figure 2.5: An integrated system with force-sensing microneedle.[angel]

2.3 Needle-puncture force detection

In retinal vein cannulation (RVC) surgery, in addition to the accuracy of the insertion of the vessel, another important issue is the angle of the insertion needle. Because the needle in the RVC procedure is usually only 42 Gauge (around 0.1 mm), when the insertion angle is not appropriate, the needle can easily be bent or even broken because of the high contact force. This not only raises the cost of the procedure, but also poses a risk to the patient's eyes during drug delivery.

Berk Gonenc at Johns Hopkins University has in 2015 developed an integrated system with force-sensing microneedle[angel]. The system can sense the puncture force during the insertion of the needle towards the vein. The needle is bent 45° to approach the vein at a constant angle at 30° during the insertion. An experiment with vinyl shows that at this setting the puncture force is around $20 \sim 25$ mN.

3 SOFA based puncture force detection

This chapter will firstly introduce the simulation framework SOFA and its forces solver, since the force solver is highly relevant to our experiment. Then in section 3.3, three kinds of models in SOFA are presented and especially the selection of force models is discussed among three options. In section 3.4 all the details of the needle puncture experiment based on SOFA will be covered.

3.1 Introduction to SOFA framework

SOFA is an Open-Source-Framework-Architecture primarily targeted at real-time simulation, with an emphasis on medical simulation[7]. It decomposes a complicated simulation scene into independently and organized nodes. Each node encapsulates several simulation features, such as degree of freedom, forces, constraints, collision algorithm, and linear solvers. The sofa was originally designed to verify the effectiveness of various algorithms, and now it has benefited several multinational companies and has hundreds of thousands of downloads.

3.2 Constraint forces solver in SOFA

SOFA allows the use of Lagrange multipliers [6] to handle complex constraints, such as contacts and joints between moving objects that can not be straightforwardly implemented using projection matrices P . They may be combined with explicit or implicit integration. Each constraint depends on the relative position of the interacting objects, and on optional parameters, such as a friction coefficient:

$$\begin{aligned}\Phi(x_1, x_2, \dots) &= 0 \\ \Psi(x_1, x_2, \dots) &\geq 0\end{aligned}\tag{3.1}$$

where Φ represents the bilateral interaction laws (attachments, sliding joints, etc.) whereas Ψ represents unilateral interaction laws (contact, friction, etc.). These functions can be non-linear. The Lagrange multipliers are computed at each simulation step. They add force terms to explicit ODE solvers:

$$\begin{aligned}A_1 \delta v_1 &= b_1 + H_1^T \delta \\ A_2 \delta v_2 &= b_2 + H_2^T \delta\end{aligned}\tag{3.2}$$

where

$$\begin{aligned} H_1 &= \left[\frac{\delta\Phi}{\delta x_1}; \frac{\delta\Psi}{\lambda x_1} \right] \\ H_2 &= \left[\frac{\delta\Phi}{\delta x_2}; \frac{\delta\Psi}{\lambda x_2} \right] \end{aligned} \quad (3.3)$$

Matrices H_1 and H_2 are stored in the *MechanicalState* of each node. Thus, when the constraint applies to a model that is mapped, the constraints are recursively mapped upward like forces to be applied to the independent degrees of freedom [5]. Solving the constraints is done by following these steps:

Step 1, Free Motion: interacting objects are solved independently while setting $\lambda = 0$. Free motion are obtained for each object.

Step 2, Constraint Solving: The constrained equations can be linearized and linked to the dynamics. The value of λ can be computed using a projected Gauss-Seidel algorithm that iteratively checks and projects the various constraint laws contained in Ψ and Φ .

Step 3, Corrective Motion: when the value of λ is available, the corrective motion is computed:

$$\begin{aligned} x_1^{t+h} &= x_1^f + h\delta v_1^c && \text{with} && \delta v_1^c = A_1^{-1}H_1^T\delta \\ x_2^{t+h} &= x_2^f + h\delta v_2^c && \text{with} && \delta v_2^c = A_2^{-1}H_2^T\delta \end{aligned} \quad (3.4)$$

An *AnimationLoop*, typically placed at the top of the graph of SOFA, has the role of imposing this new scheduling to the rest of the graph. During each simulation step, the collision forces can be computed and updated.

3.3 SOFA models related to puncture experiments

In SOFA, each object can be simulated using three different models: visual model, collision model, and deformation model. These three models are linked together with mapping function. This section will give details on the three models of the two objects in the needle puncture experiment: the micro-needle and the vessel on the retinal.

3.3.1 Visual models

A visual model is dedicated to the visual rendering process. Compared with the other two models, the visual model contains usually more nodes and more detailed geometry and thereby behaves much smoother.

Here in our experiment, both of the micro-needle and the vein are modeled in SOLIDWORKS.Edu version[17]. As figure 3.2 shows, the total length of needle is around 30mm, and the ending part of the needle was bent nearly 30 degrees like how Gonenc B. did [3]. Besides the tip of the needle was also sharpened up, in order to facilitate the entry of the needle into the blood vessel. Totally it contains more than 4000 nodes.

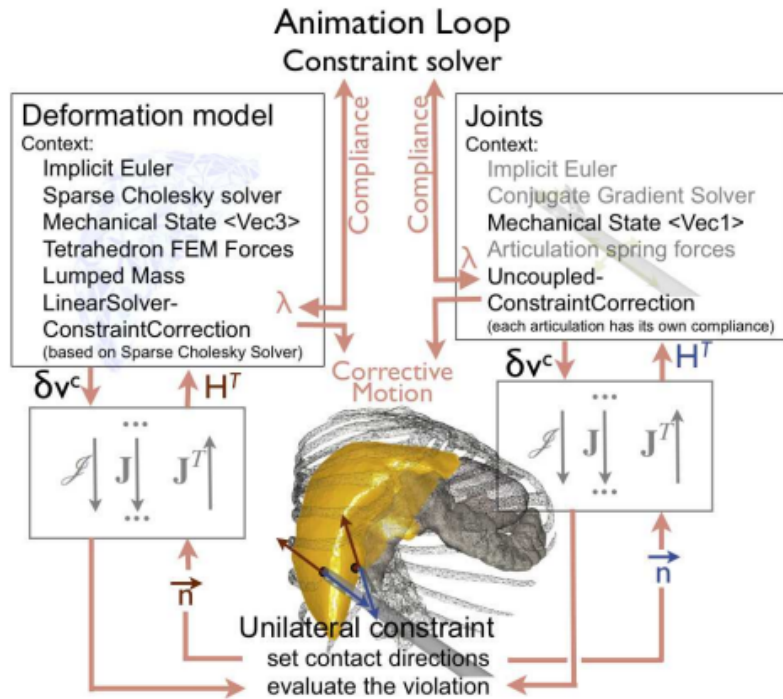


Figure 3.1: SOFA: The whole process of constraint solver and collision force update

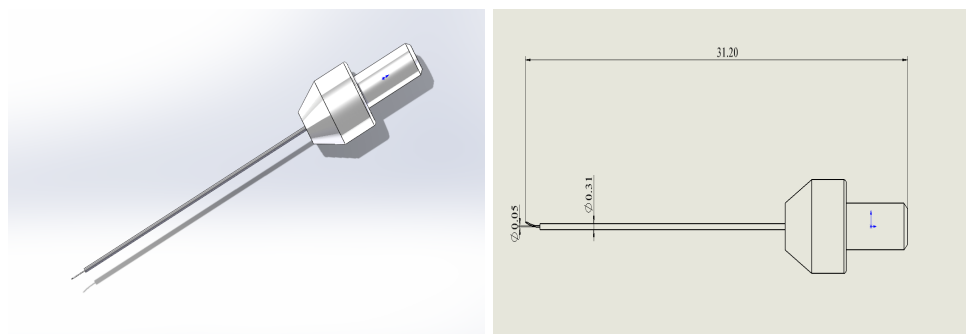


Figure 3.2: Visual model of Micro-needle

3 SOFA based puncture force detection

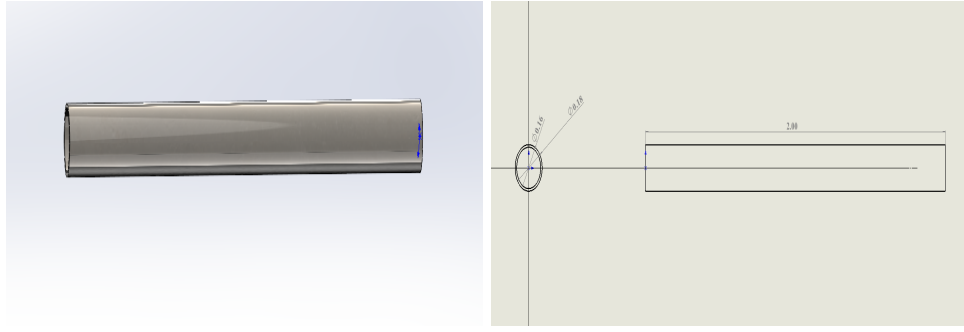


Figure 3.3: Visual model of retinal vessel

And as for the visual model of the vessel, according to the information about retinal vessels provided by Tel Aviv University(Israel), the outer diameter is 0.18 mm and the inner diameter is 0.16 mm . For simplicity, only a small portion of the vessel was selected, so the vessel was designed as a hollow cylinder, rather than a curved vessel as a whole. It contains a total of around 80000 nodes shown by figure 3.3.

Both models are transformed from .SLDPRT model to .OBJ file via 3D scanning and mesh construction in SOLIDWORKS. Then the .OBJ files can be loaded into SOFA. After adjusting the view parameters, such as color and transparency, the SOFA interface with visual models looks like figure 3.4

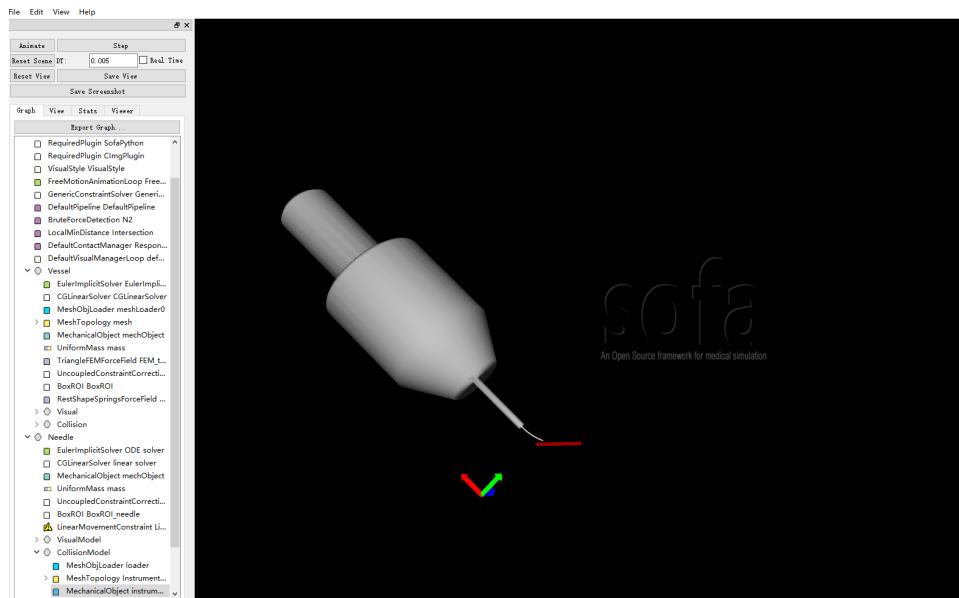
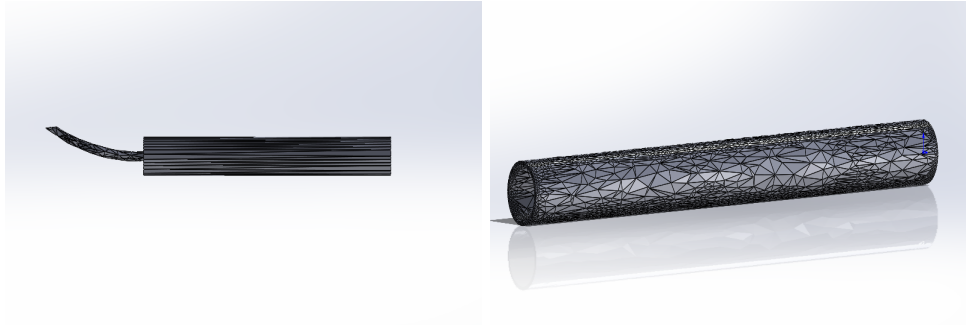


Figure 3.4: The visual models of needle puncture experiment in SOFA



(a) Collision model of needle

(b) Collision model of vessel

Figure 3.5: Collision models

3.3.2 Collision models

In order to adapt the models to the data structure of the different collision algorithms, a separate collision model is employed for each object. This model is similar to an internal or visual model, except that its topology and its geometry can be stored in for collision detection. A trade-off between precision and efficiency is that visual model usually takes a much smoother model and collision model is coarser than an internal mesh.

In our case, the collision model of vessel is the same 3D model as the visual model, just the nodes are reduced from 80000 to 40000, so that the model will look a little angular not so smooth. And as for the micro-needle, because only the end part of the needle takes part in the collision with vessel, only the tip of needle is modeled for collision detection and other parts are ignored during the meshing phase. So the total nodes of model are greatly reduced from 4000 to 1000 (Figure3.5).

3.3.3 Force models

The force model is used to represent an object's internal mechanical behavior, which may be mainly computed using Finite Element Method (FEM). The geometry of this model is optimized for the computation of internal forces, typically using a reduced number of well-shaped topologies for speed and stability. Several topologies are supported in SOFA and can be loaded for computation3.6. Here we select three possible topologies as options that are commonly used in FEM method, and finally select the best one for experiment. The criterion is the similarity of their force curve during the simulation experiment with the force curve, that is obtained in real puncture experiment executed by Gonenc B[3]. In the SOFA simulated experiment, the vessel is located in the rigid floor, and the needle executes the insertion movement in 30 °. The solved collision force data are stored during the process, analysed and finally visualized. Besides, the total number of nodes of three models is all almost the same, around 10000.

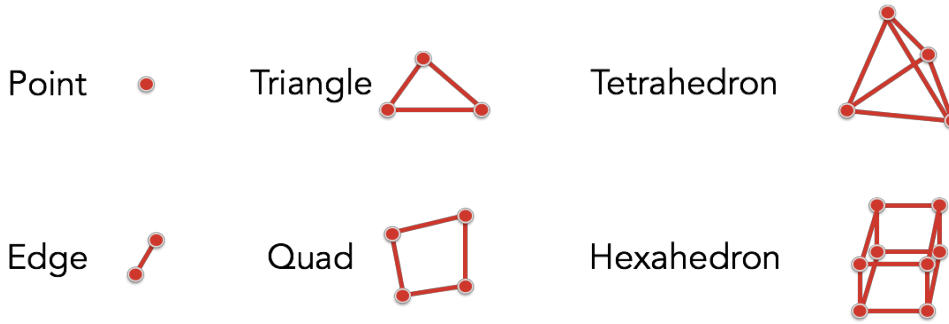


Figure 3.6: Supported topologies in SOFA

Grid FEM force field

In SOFA, the bounding box where the retinal vessel is located is divided into (nx, ny, nz) small squares, and each small square is then meshed into tetrahedron elements. The meshes and the final force curve of grid FEM force field is shown in figure 3.7. The force curve that is directly extracted from the solver is mess and steep, so sliding windows smooth method in Scikit-learn library is used for all three force models to post-process the force data.

Triangular FEM force field

The triangular meshes can be generated from a .stl surface file in SolidWorks. Then the generated .obj file which contains the triangular meshes can be loaded into SOFA. Figure 3.8 shows the triangular FEM force field in SOFA and the post-processed force curve.

Tetrahedron FEM force field

Tetrahedron is the most popular topology because of its less distortion of mesh and low computational costs. Given a .stl surface file, tetrahedral meshes can be generated via Gmsh[8]. Figure 3.9 shows the tetrahedron FEM force field in SOFA and the post-processed force curve. Given all three force curves and the force curve from the experiment with a real micro-needle and real vinyl [3] as ground truth (Figure 3.10), we observe that the peak values of all curves are at around 20 mN, which proves that the FEM methods in SOFA and its settings are accurate compared with the ground truth. Also, compared with the other two curves, the curve of tetrahedron FEM model is much smoother and less mess or bumps, especially after the needle punctures the vessel the forces stay still, whose property is basically same as the ground truth.

For the above reasons, we choose the tetrahedron FEM model as the final choice.

3.4 SOFA based puncture experiments

After having decided the three models of two objects: the micro-needle and the retinal vessel for now, a SOFA based puncture experiment is possible for now. GenericConstraintSolver

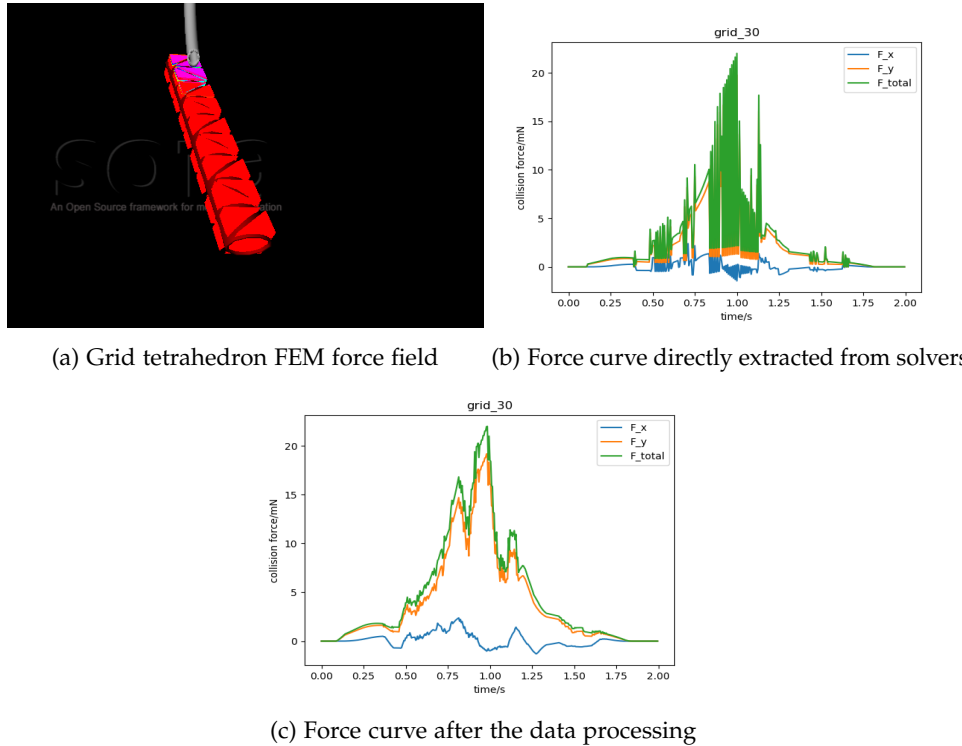


Figure 3.7: Grid FEM meshes and the force curves of it

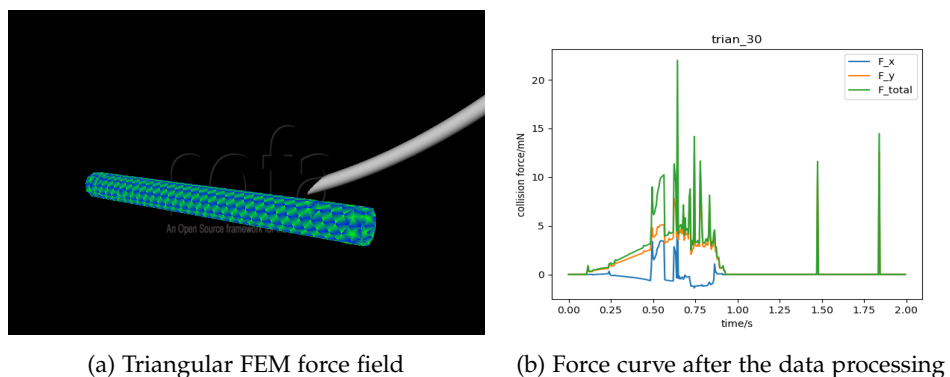


Figure 3.8: Triangular FEM meshes and the processed force curves.

3 SOFA based puncture force detection

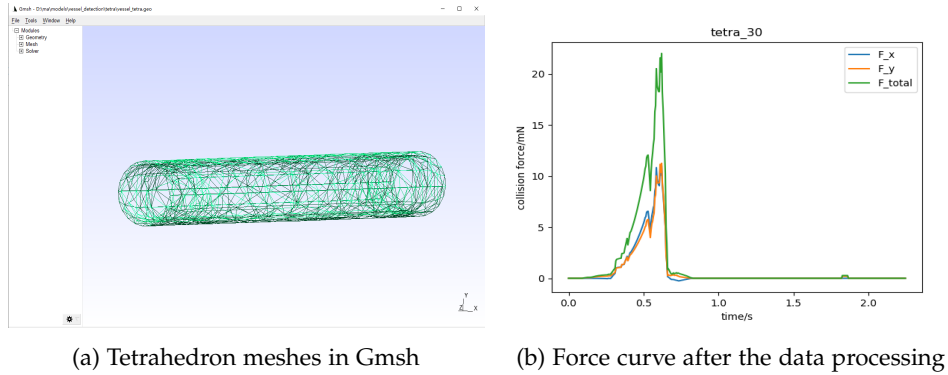


Figure 3.9: Tetrahedron FEM meshes and the processed force curves.

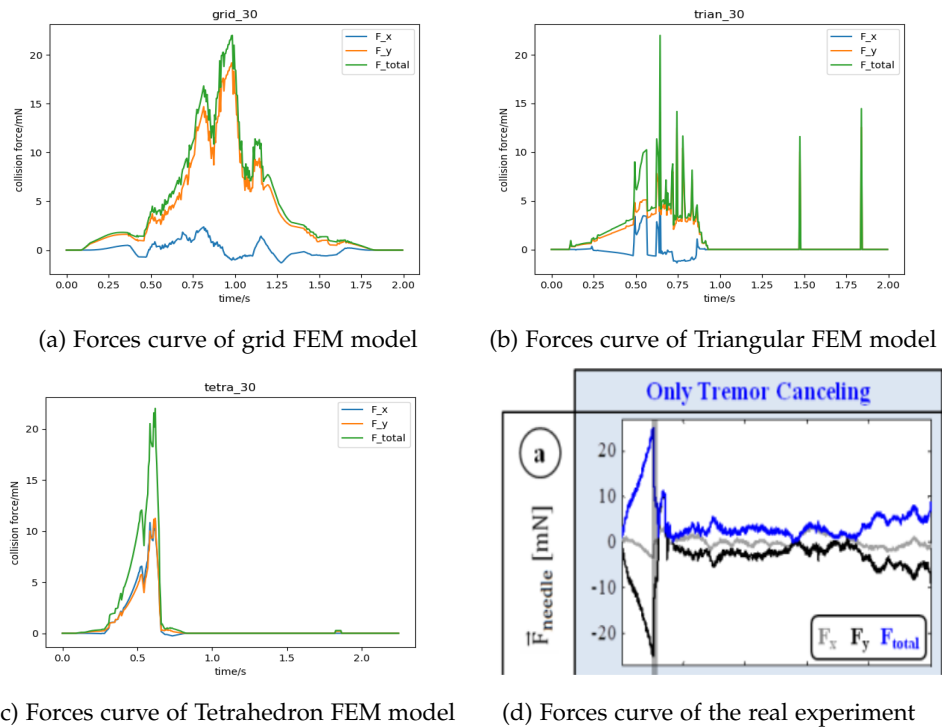


Figure 3.10: Curves of three kinds of FEM models and ground truth

is used as the force solver, and for collision detection we used BruteForceDetection and LocalMinDistance collision detection algorithm. For more details please refer to the codes.

Since the experiment was designed to investigate mainly the relationship between puncture angle and puncture force, we recorded and visualized the corresponding puncture force curves at 15, 30, 45, and 60 degrees as the puncture angles, respectively, and tried to obtain conclusions. Figure 3.11 shows how the total experiment scene looks like, and Figure 3.12 presents the final post-processed results of experiments with 4 different insertion angles.

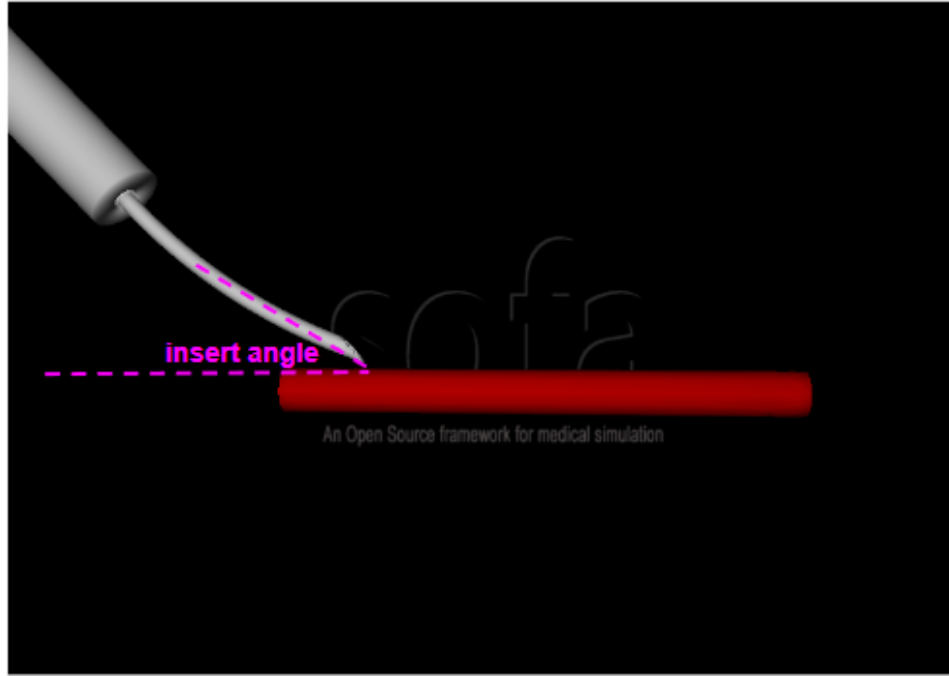


Figure 3.11: An example of puncture experiment in SOFA

3.5 Conclusion

Observing the experimental curves, we can summarize two points:

- At all angles, the contact force curve always increases as the contact depth between the needle and the vessel increases. When the needle penetrates the vessel, the contact force reaches its maximum value, called the puncture force, and then the contact force decreases sharply and approaches 0.
- The penetration force required by the needle is maximum at an insertion angle of 15 degrees, which is about 30 mN. The penetration force decreases as the angle of needle insertion increases, and only about 15 mN is required at 60 degrees.

In the following sections, a mechanics-based explanation and some discussion of the application to clinical practice will be given.

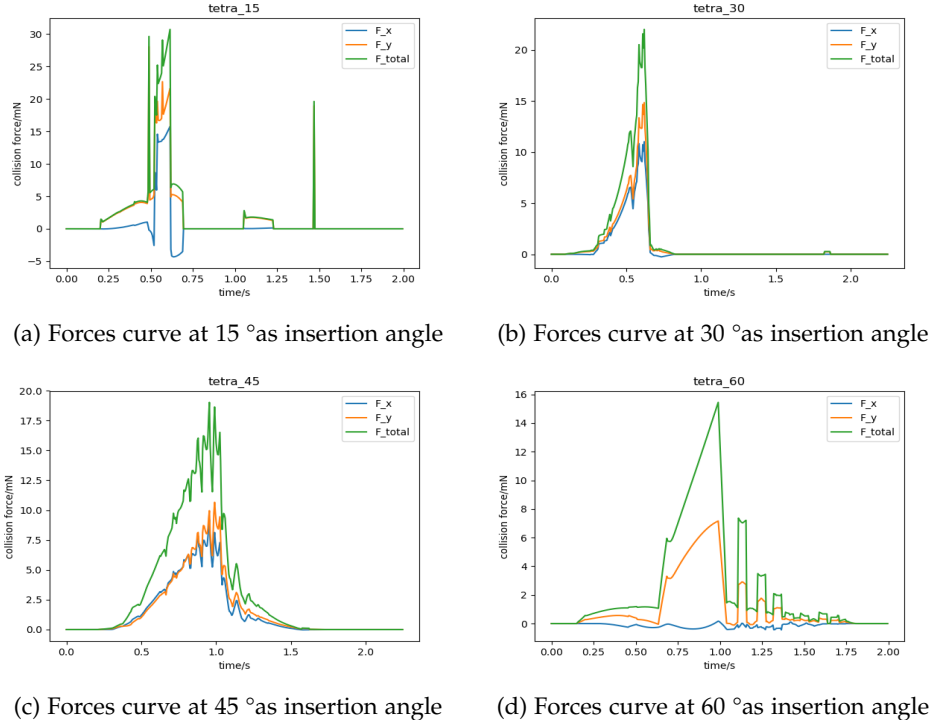


Figure 3.12: Experiments result of 4 different insertion angles

3.6 An mechanics-based explanation

The whole process of micro-needle puncturing vessels is considered as applying normal stress on vessels. And the mechanics of blood vessel are considered to be viscoelastic.[14] Viscoelasticity is the property of materials that exhibit both viscous and elastic characteristics when undergoing deformation. Figure 3.13 shows the stress-strain curve of viscoelastic material. The strain increases proportionally with stress at first stage. Then the young's modulus changes a little bit in some range. When the strain exceeds some threshold value ϵ_0 , the vessel undergoes fractures and is punctured by the needle.

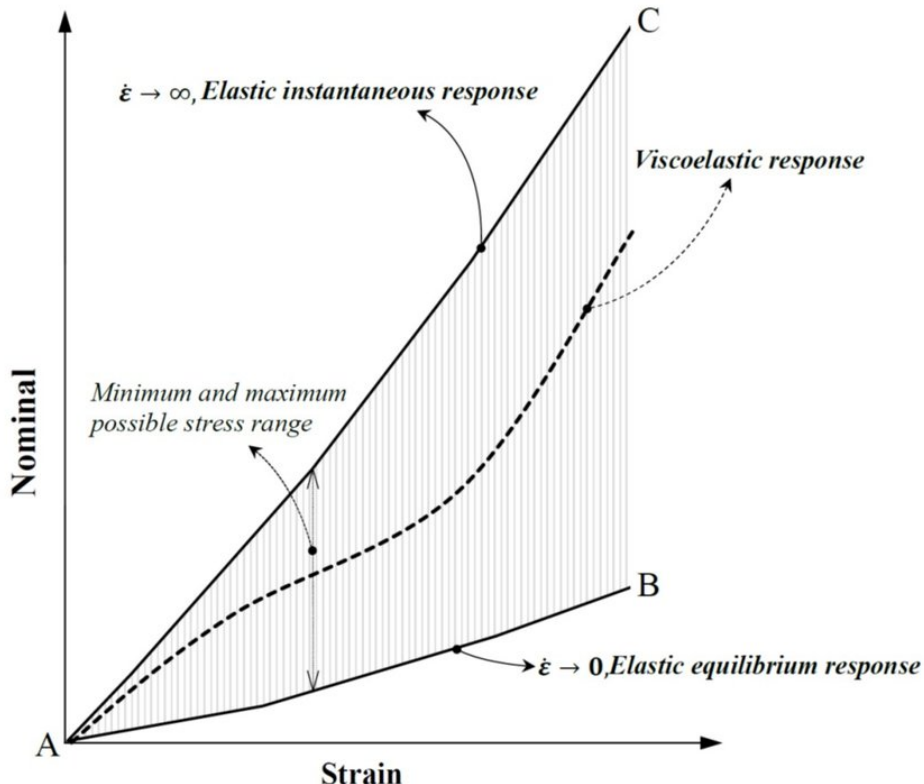


Figure 3.13: Stress-strain curve of viscoelastic material.

A simplified mechanics model is described in figure 3.14, where α is the insertion angle, σ is the nominal stress and ϵ is the strain.

$$\begin{aligned}
 F_y &= F_{total} * \sin(\alpha) \\
 \sigma &= \frac{F_y}{A_0} \\
 \epsilon &= \frac{\sigma}{E}
 \end{aligned} \tag{3.5}$$

When the vessel is punctured, $\epsilon > \epsilon_0$

Given a constant ϵ_0 as threshold value, with α increases, the required stress σ_0 and $F_{total,0}$

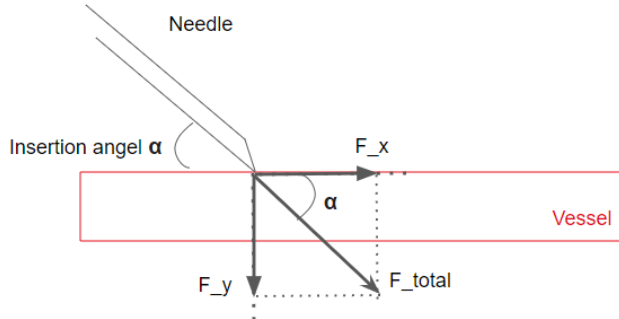


Figure 3.14: Simplified mechanics model of the puncture experiment

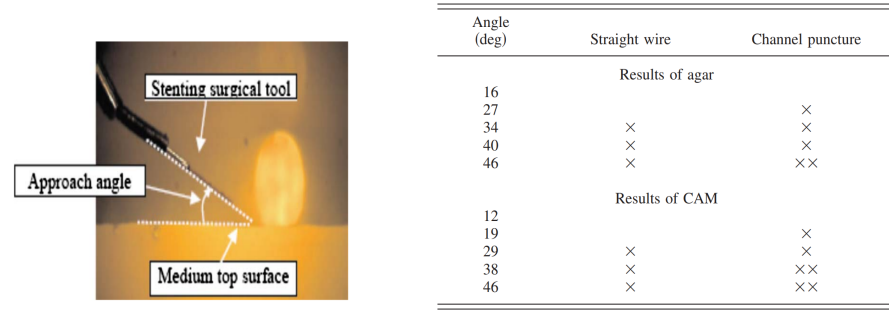
as puncture force are consequently decreased. Here the vessel fracture is assumed to depend only on the nominal strain. Besides, as the insertion angle becomes bigger, the needle is more closer to vertical, so that the contact area A_0 between needle and vessel is obviously smaller. According to equation 3.5, the required puncture force with bigger insertion angle could also be lighter than the ones with smaller insertion angle.

3.7 Validation and Discussion

W. Wei et al.[20] in 2010 used stenting deployment unit (SDU) as a potentially revolutionary surgical treatment for retinal vascular occlusions that do not permanently resolve using pharmaceutical treatment. With SDU they also did puncture experiments on both agar and chick chorioallantoic membranes (CAM).With changing angles, whether the channel is punctured and whether the stenting is still straight after puncture is recorded. Figure 3.15 shows the experiment setup and the final result.

For understanding the result table, in the channel vessel puncture columns, single check means the needle pokes through the top surface and double checks mean the needle poke through both the top and the bottom surfaces. In the straight wire columns, single check means the SDU is still straight after puncture while no check means that the SDU is bending due to impact and contact. Therefore, an important observation is that on both agar and CAM, with increasing insertion angle, the SDU is more possible to undergo less collision and therefore be straight. Another finding is that when insertion angle goes up, the experiment material is more easily to get punctured, however the needle poke also tends to more likely pass through both the top and the bottom surfaces, and causes more traumas.

So combining the observations from [20] and the conclusions from section 3.5, we can summarize that the optimal insertion angle of micro-needle into retinal vessel should be



(a) Setup for SDU puncture experiment

(b) Result of puncture on agar and CAM

Figure 3.15: Puncture experiment setup and result

between 25° and 30° . If the angle is too small, the puncture force is so large, that the needle is easily bent, and the wound opening is also wide. If the angle is too large, it is easy to accidentally puncture the lower wall and cause traumas.

4 SOFA based retinal surgery simulation system

In SOFA, each scenario is composed of many components and these components are represented by nodes. In our retinal surgery simulation scenario, mainly 4 kinds of nodes are included: 3D Models of objects such as needle and eyeball(section 4.1), controller nodes to control the handle with the movement of the micro-needle(section 4.3), trauma detection node(section 4.4) and some visual nodes(section 4.5).

4.1 Models

4.1.1 Eyeball

Given that the eye is a relatively complex structure. In order to achieve as high a level of simulation as possible and to try to recreate the eye structure, instead of directly modeling a complete eyeball model, we decompose the eye into several structures in the simulation system: the white of the eye, the sclera, the iris and the retinal vessels. In all three visual models, separate texture images are added for each visual model4.1.

4.1.2 Retinal Vessel

We illustrate the blood vessel separately from the eye because the blood vessel is a separate model in the modeling process. In Solidworks, it is obtained by sweeping and projecting on the sphere of eye white part as a reference. Therefore its nodes number and FEM properties can be adjusted separately. The shape and orientation of the blood vessels were modeled with reference to Figure 4.2, preserving the aorta of the retina and ignoring some narrow branching arteries, and it contains a total of 100 nodes.

4.2 Transformation

To prevent potential damage or trauma on the eyeball caused by the micro-needle, two trocars are usually inserted on the operated eyeball, which provides a physically constrained point for the needle. Hence, the micro-needle is able to move along or rotate around the incision point. Such movement is called Remote Center of Motion (RCM)[21].

The center point in our case is just where the trocar locates. In order to achieve such RCM in SOFA simulation framework, a trick here is to locate the trocar exactly in the global coordinate origin. Since a property in SOFA frame is that the movement of object can only be

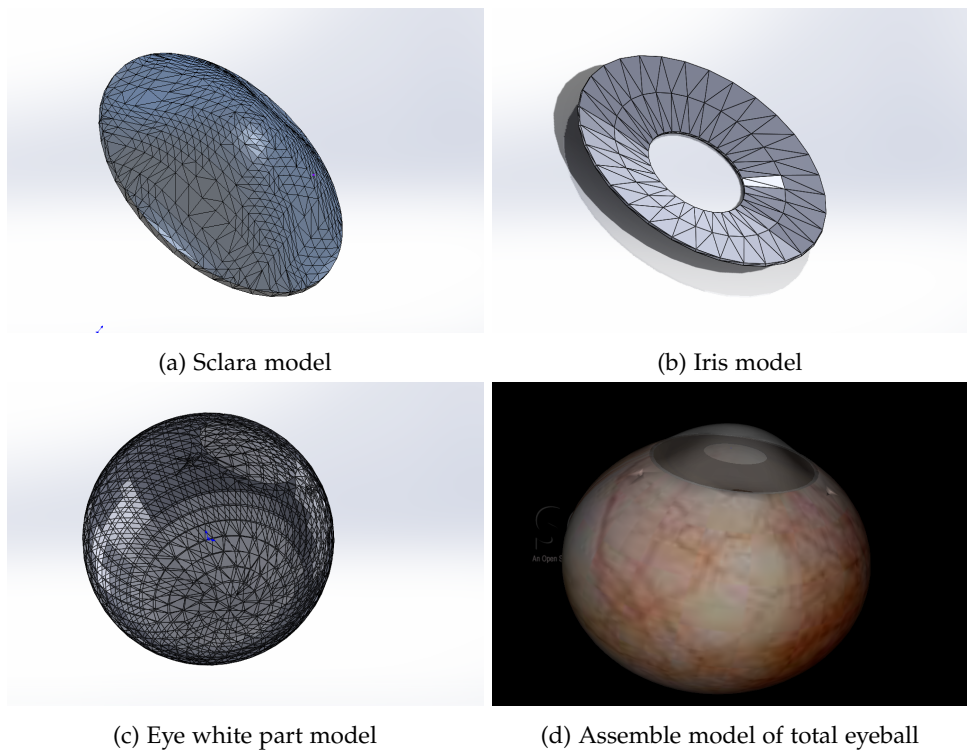


Figure 4.1: Separate parts models and the total assemble

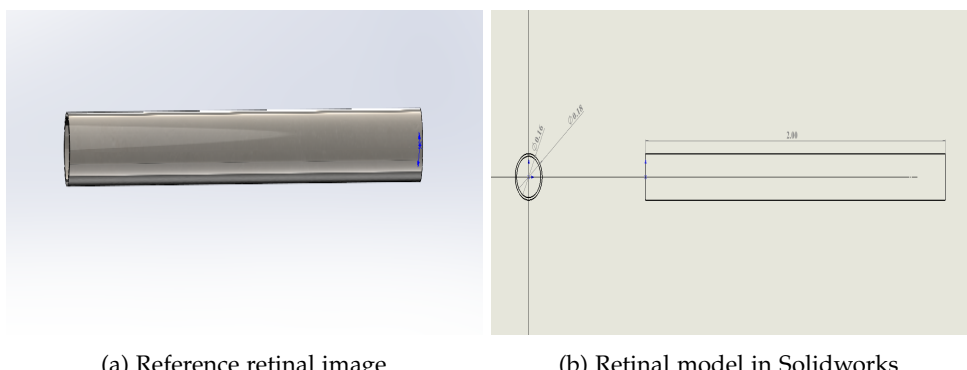


Figure 4.2: Reference retinal image and retinal model

controlled in global coordinate. Hence, the micro needle would rotate around the RCM point or the global origin in any case (Figure 4.3).

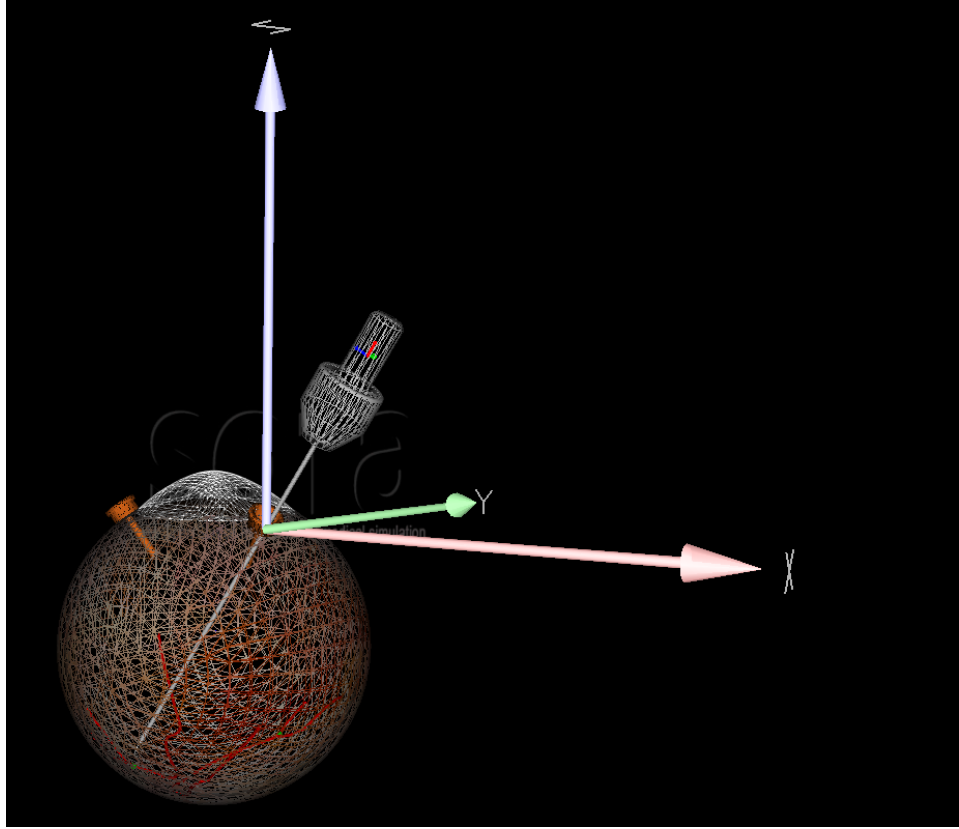


Figure 4.3: The trocar locates exactly at the global origin as RCM center

However the micro needle is supposed to rotate or translate along its own coordinate axis, therefore we need to calculate the transformation matrix R_q^p transform the movement in local coordinate q to global coordinate p . Also another property in SOFA is that the spatial rotation of objects are described in quaternions. A spatial rotation around a fixed point of θ radians about a unit axis (X, Y, Z) that denotes the Euler axis is given by the quaternion $(C, X S, Y S, Z S)$, where $C = \cos(\theta/2)$ and $S = \sin(\theta/2)$. So for more intuitive angle control, a transformation between euler angle and quaternions. A pseudo codes are provided in Algorithm 1.

4.3 Controller

As haptic devices, two controller are supported as input source to control the movement of the mirco-needle, all degrees of freedom of needle is shown in Figure 4.4.

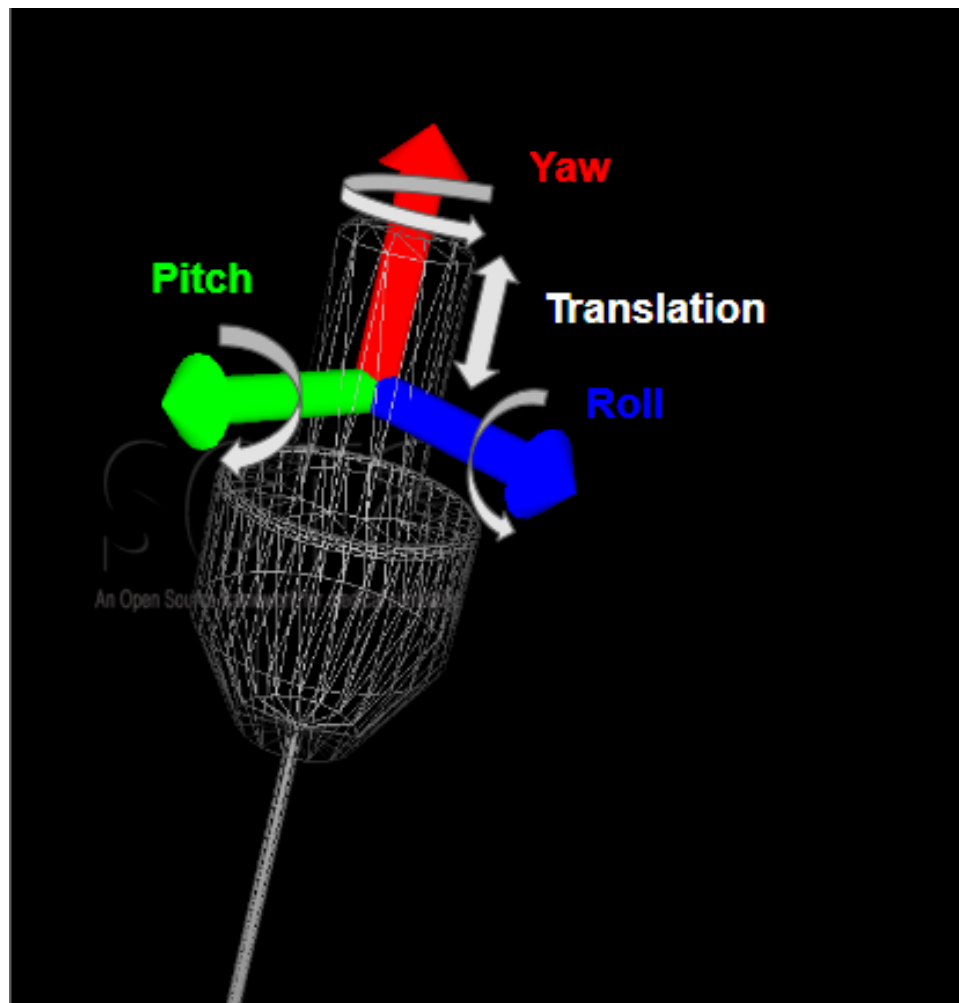


Figure 4.4: 4 DOF of needles: yaw, roll, pitch and translation

Algorithm 1 RCM control algorithm in SOFA

Require: State quaternion v , local coordinate q , global coordinate p

Ensure: Desired movement quaternion u

Calculate R_q^p

$\bar{v} = \text{QuaternionToEulerAngle}(v)$ $\triangleright \bar{v}$ is the euler description of the needle's pose

$\bar{u} = R_q^{p^{-1}} * \bar{v}$

$u = \text{EulerAngleToQuaternion}(\bar{u})$

4.3.1 Keyboard

The keyboard is an classical old-school input resource, which is easier and pretty familiar for operator.

The operator can always control the needle via pressing number keys 1 3, 4 6, 7 9 for three different rotation DOF. And by pressing number keys 8 2 translation movement can be executed, which means "insert" or "draw" in this simulation scenario.

4.3.2 SpaceMouse

While SpaceMouse as joystick, is more intuitive and convenient for the user to form a mapping relationship between controlling and movements of needle. The motion of the handle can be considered as an approximate version of the RCM motion: the connection point between the SpaceMouse handle and the SpaceMouse base can be considered as the center point, and the handle can be rotated around the center point and pushed and pulled in the vertical direction as well, which are corresponding to the 4 degree of freedoms of the needle.

Since SOFA does not naturally support the usual SpaceMouse driver, to implement the SpaceMouse controller, an communication bridge between SpaceMouse and SOFA is established by using multiprocessor communication package based on sockets protocol. Figure 4.5 shows the whole communication process between two processors.

Real time is always a concern related to sockets protocol. And the real time property was tested by evaluating the communication time from session 1.2 to session 2.2 in figure 4.5. And the results shows that communication time is shorter than a millisecond most of the time, which satisfies the real time requirement.

4.4 Trauma detection

Because the retinal surgery demands high precision of operation and the insert depth of needle in eyeball is difficult to estimate, the trauma that occurs during retinal vascular injection surgery has been a major concern and has a significant impact on postoperative recovery. Therefore, trauma detection is a necessary part of the simulation system. Figure 4.6 shows the how the trauma can be generated in the simulation system.

In our simulation system, at each simulation step the location of the needle-tip will be detected and stored. When the needle collides with the eyeball white part, the trauma could

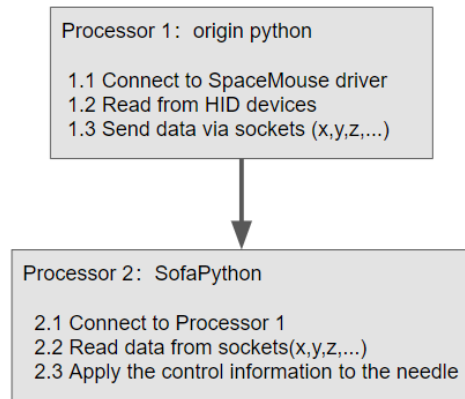


Figure 4.5: Multi-processor communication for SpaceMouse driver

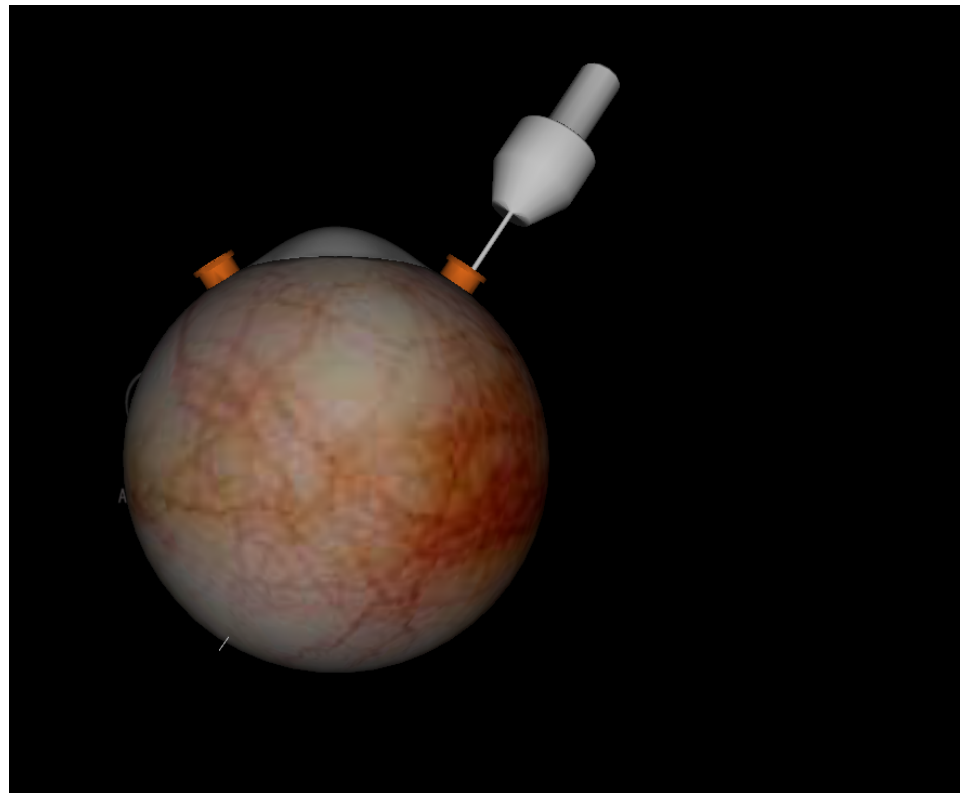


Figure 4.6: Generated trauma because of wrong depth estimate

be detected. The trauma count is not counted as once until the needle leaves the eyeball white part.

4.5 Graphic view

In performing retinal vascular cannulation (retinal vein injection), the surgeon usually performs the procedure through the screen of a microscope. The microscope can usually be adjusted in magnification to suit different surgical settings. In SOFA simulation system, the microscope is located on the top of the eyeball and provides a adjustable scope view, which is in the left-down side of GUI interface. The operator could press "PgUp" to increase and "PgDn" to decease the magnification.

Besides, some information about operation time, trauma numbers and movement step size are provided in the right side of GUI interface. Figure 4.7 shows the complete simulation interface.

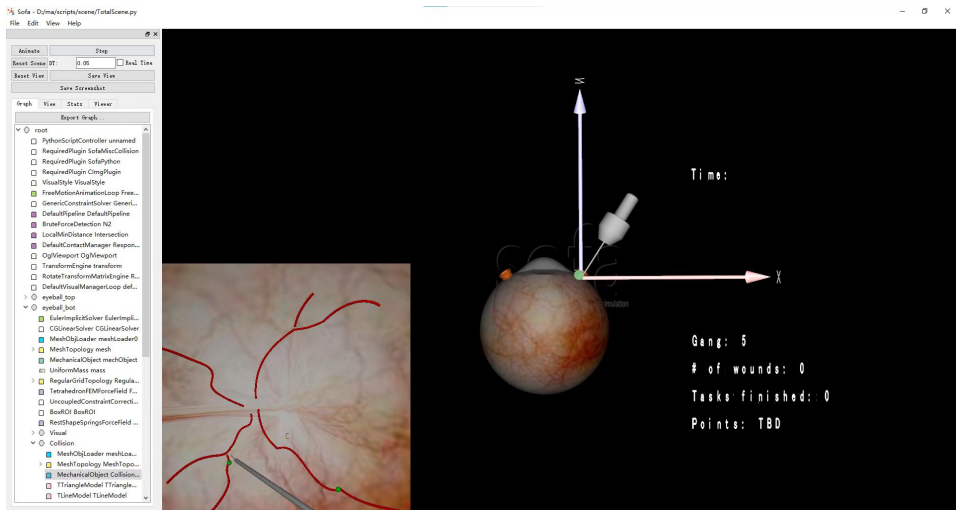


Figure 4.7: Generated trauma because of wrong depth estimate

4.6 Experiment

We designed the retinal vein injection simulation experiment with three motives: 1. to study the effectiveness of the simulation system 2. to derive the learning curve on the simulation system 3. to compare the learning curves of two different control methods (SpaceMouse and Keyboard).

4.6.1 Task description

In this simulated scenario, operators were assigned a retinal vascular injection task.

A total of two blood vessel branches need to be injected with thrombolytics by operators, which are marked with green spheres in the scene. By operating the keyboard and handle (SpaceMouse) respectively, the operators can control the four-degree-of-freedom movement of the injection needle in the simulation environment (three rotations, one translation). Move the needle to the branch of the blood vessel where the thrombolytic agent needs to be injected, and wait for one second to complete the injection. At this time, the ball turns red, which means that the thrombolysis is successful and the blood vessel is healed and turns red.

When two vascular injection tasks are completed separately, the entire task is considered complete. Throughout the process, the simulation environment detects whether the needle collides with other parts of the retina, causing trauma. When both tasks are completed, the evaluation system will judge the quality of the surgical operation, and give feedback and score based on the operation time and the number of trauma.

We hope that such a simulated experimental task can not only improve the proficiency and confidence of ophthalmologists in performing retinal surgery with bare hands, but also by changing the mapping relationship of control, doctors can be more familiar with the operation of the WeiFeng retinal vein injection robot, so that retinal surgery can benefit from the robot's high-precision motion.

4.6.2 Evaluation system

In order to evaluate the performance of operator during the tasks and provide a feedback, an evaluation system is also implemented based on the operation time and operation quality. The calculate equation of performance points is:

$$\begin{aligned} \text{Performance points} &= 100 - \max(50, \text{ceiling}((t - 120)/10)) - N * 10 \\ \text{Final Points} &= \max(0, \text{Performance points}) \end{aligned} \quad (4.1)$$

Where t is duration time and N is the number of trauma caused by unsuitable operation. And 120 is an empirical value of the average operating time. The most points deduced because of operation time is limited to only 50, considering it is also a very safe surgical option to ensure the quality of the operation without regard to the operation time.

4.6.3 Experiment settings

Six non-medical undergraduates, who had neither previously used the retinal surgery simulator nor any experience of retinal surgery operation, were invited to participate in the study in June 2022.

Each participant was given six tasks as workload, where each task contained two injection subtasks, as 4.6.1 shows. Before the start of the formal task, each participant was given 10 minutes of practice time to familiarize with the controller and the simulation system to ensure that the system would not be down due to unexpected activities. During the formal task, each participant crossed the order of the keyboard and SpaceMouse handle to record the time and number of trauma to complete each task. Half of the participants (Group 1) started with Keyboard as input method (tasks order: [Keyboard, SpaceMouse, Keyboard, SpaceMouse,

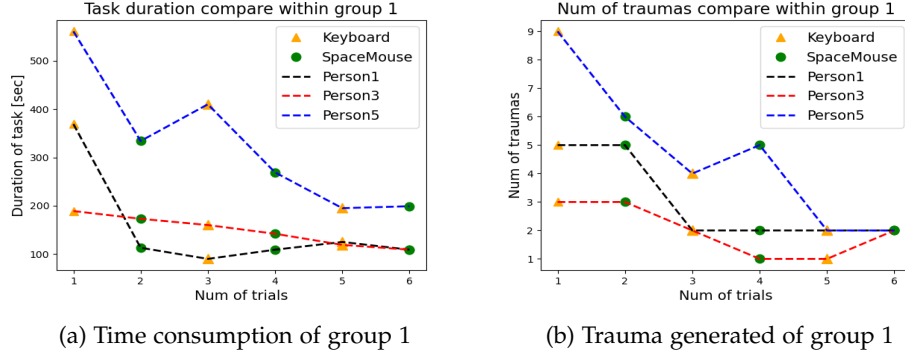


Figure 4.8: Experiments results of group 1

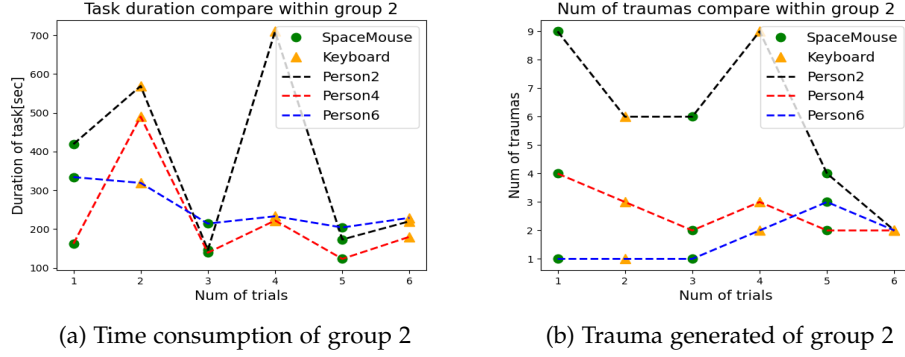


Figure 4.9: Experiments results of group 2

Keyboard, SpaceMouse]) while the other half (Group 2) used SpaceMouse as the first task. The purpose of this crossover input approach was to ablate the effect of each participant's previous familiarity with the input methods (Keyboard and SpaceMouse) on the results of the experiment. For example, if a participant is familiar with keyboard operation, such as a PC-gamer, he or she can expect to perform better on the keyboard than on the SpaceMouse.

4.6.4 Experiment results

Figure 4.8 and Figure 4.9 and shows the experiment results of totally 6 tasks for each participant in group 1, who starts with keyboard and group 2, who starts with SpaceMouse.

4.6.5 Experiment conclusion

Regarding to the learning curve for both time and trauma, all participants has shown an obvious decreasing trend in task duration and number of generated trauma generally. Most participants would spend more than 300 seconds at first, while it costs only around 200 seconds finally. And as far as the trauma is concerned, almost all the participants generate

many wounds at first because of unfamiliarity with the controller. However after training for several times, most could keep generating only two trauma during the operation.

By comparing the two different input methods, it could be observed that the duration of the tasks operated by SpaceMouse is generally shorter than the tasks operated by keyboard, though all tasks operated by both controller take fewer time as the participants become more familiar with. A possible explanation is that compared with keyboard, SpaceMouse is more intuitive in the sense of mapping relationship between controller and needle movement. The motion of the handle can be considered as an approximate version of the RCM motion (mentioned in section 4.3.2) just like the micro-needle in retinal vein injection operation.

And regarding to the number of trauma, the difference between two input methods are not obvious. It may be because the keyboard is discrete control, it is easier to control the speed of the needle, when the micro-needle tries to approach the targets points step by step. However, SpaceMouse controlling is continuous, when trying to approach the target point, it may be difficult to control the speed of the needle movement, so that the needle may punctured the retina at once, which may cause puncture trauma in retina.

5 Limitations

In this work, the first simulation system specifically for RVC surgery is designed and implemented. In view of the high difficulty and risk of retinal surgery, we hope that such a simulated experimental task could improve the proficiency and confidence of ophthalmologists in performing retinal surgery with low time and economic costs. In addition, the relationship between the insertion angle of micro-needle into retinal vessel and the puncture force is studied. And the optimal insertion angle is supposed to be between 25° and 30° considering that the needle could also accidentally puncture the lower vessel wall as well.

However, there are some inadequacies to be improved in this work due to the limited time. For example, when studying the insertion angle of the needle, more accurate results will be obtained if the topological model of the needle is also included. In addition, only six participants were invited to conduct the experiments in the simulation system due to time constraints. The experimental results should be more convincing if more people can participate in the experiment and provide valid data.

6 Conclusion

In this work, the first retinal vein injection (RVJ) simulation system, to our best knowledge, is designed and implemented. Based on SOFA (Open-Source-Framework-Architecture), the simulation includes mainly two objects: eyeball and the micro-needle. And each object contains visual model, collision model and force model thanks to the mapping function feature in SOFA. Two controller, keyboard and SpaceMouse, are supported to control the 4 DOF movement of the micro-needle. To obtain the learning curve of operating the simulated RVC operation and study the difference of the efficiency and confidence of the two methods, six participants were invited to the experiments. It was concluded through experiments that compared with keyboard, the tasks with SpaceMouse were evaluated usually better because it is more intuitive in the sense of mapping relationship between controller and needle movement.

Additionally, based on the Finite-Element-Method simulation system, the relationship between insertion angle of the micro-needle and puncture force was investigated. At first three different mesh types are compared, the one that best fits the real situation is selected. Experiments show that within a certain range, the larger the insertion angle, the smaller the puncture force required to puncture the vessel. Finally a theoretical mechanical model is given to explain such relationship.

In view of the high difficulty and risk of RVC surgery, we hope the SOFA based retinal surgery simulation system could improve the proficiency and confidence of ophthalmologists in performing retinal surgery with low time and economic costs.

List of Figures

1.1	Normal human retinal and retinal vein occlusion	1
1.2	Pig eyes v.s. human eyes	2
1.3	SpaceMouse: 6 DOFs joystick	4
2.1	Parallel Coupled Joint Mechanism (PCJM) used in TUM-invented robots RAMS	6
2.2	First-In-Human Robot-Assisted Subretinal Drug Delivery with Preceyes Robots	7
2.3	Eyesi Simulator and retinal surgery training modules	8
2.4	A low-cost complete eyeball for retinal surgery[13]	9
2.5	An integrated system with force-sensing microneedle.[angel]	9
3.1	SOFA: The whole process of constraint solver and collision force update	12
3.2	Visual model of Micro-needle	12
3.3	Visual model of retinal vessel	13
3.4	The visual models of needle puncture experiment in SOFA	13
3.5	Collision models	14
3.6	Supported topologies in SOFA	15
3.7	Grid FEM meshes and the force curves of it	16
3.8	Triangular FEM meshes and the processed force curves.	16
3.9	Tetrahedron FEM meshes and the processed force curves.	17
3.10	Curves of three kinds of FEM models and ground truth	17
3.11	An example of puncture experiment in SOFA	18
3.12	Experiments result of 4 different insertion angles	19
3.13	Stress-strain curve of viscoelastic material.	20
3.14	Simplified mechanics model of the puncture experiment	21
3.15	Puncture experiment setup and result	22
4.1	Separate parts models and the total assemble	24
4.2	Reference retinal image and retinal model	24
4.3	The trocar locates exactly at the global origin as RCM center	25
4.4	4 DOF of needles: yaw, roll, pitch and translation	26
4.5	Multi-processor communication for SpaceMouse driver	28
4.6	Generated trauma because of wrong depth estimate	28
4.7	Generated trauma because of wrong depth estimate	29
4.8	Experiments results of group 1	31
4.9	Experiments results of group 2	31

List of Figures

Bibliography

- [1] 3DConnexion. *SpaceMouse*. URL: <https://3dconnexion.com/uk/spacemouse/>.
- [2] Guerrouad A and Vidal P. "stereotaxical microtelemanipulator for ocular surgery". In: *Annu Int Conf IEEE Eng Med Biol Soc* (1989).
- [3] Gonenc B et al. "Force-Based Puncture Detection and Active Position Holding for Assisted Retinal Vein Cannulation." In: *IEEE SICE RSJ Int Conf Multisens Fusion Integr Intell Syst 2015* (2015), pp. 322–327. doi: 10.1109/MFI.2015.7295828.
- [4] Zevin B, Aggarwal R, and Grantcharov TP. "why is it still not the standard in surgical training?" In: *J Am Coll Surg* 218:294 (2014).
- [5] Christian Duriez et al. "Contact skinning." In: *n Eurographics conference (short paper)* (2008).
- [6] Christian Duriez et al. "Realistic haptic rendering of interacting deformable objects in virtual environments." In: *IEEE Transactions on Visualization and Computer Graphics* 12 (2006), pp. 36–47.
- [7] François Faure et al. *SOFA: A Multi-Model Framework for Interactive Physical Simulation*. Springer, 2012.
- [8] Gmsh. *Gmsh*. URL: <https://gmsh.info/>.
- [9] Robert A. MacLachlan et al. "Micron: An Actively Stabilized Handheld Tool for Micro-surgery". In: *IEEE Transactions on Robotics* 28.1 (2012), pp. 195–212. doi: 10.1109/TRO.2011.2169634.
- [10] M. Ali Nasseri et al. "The Introduction of a New Robot for Assistance in Ophthalmic Surgery". In: *35th Annual International Conference of the IEEE Engineering in Medicine and Biology and Biology Society (EMBC'13)*. IEEE Press, 2013.
- [11] Valentine R, Padhye V., and Wormald PJ. "Simulation Training for Vascular Emergencies in Endoscopic Sinus and Skull Base Surgery." In: *Otolaryngol Clin North* 49.877 (2016).
- [12] V. Radeck et al. "The learning curve of retinal detachment surgery." In: *Graefes Arch Clin Exp Ophthalmol* 259.10 (2021), pp. 2167–2173. doi: <https://doi.org/10.1007/s00417-021-05096-1>.
- [13] James Rice. "Making a low-cost retinal surgical simulator." In: *Community Eye Health* 32.106 (2019), pp. 34–35.
- [14] Nerem RM. "Tissue engineering a blood vessel substitute: the role of biomechanics." In: *Yonsei Med J* 41 (2000), pp. 735–739.

Bibliography

- [15] Haag-Streit Simulation. *Eyesi*. URL: <https://www.vrmagic.com/medical-simulators/eyesi-surgical>.
- [16] SOHU. *First case in Sichuan where pig corneas were successfully transplanted into human body*. 2016. URL: https://www.sohu.com/a/68934864_116237.
- [17] DASSAULT SYSTEMES. *Solidworks*. URL: <https://www.solidworks.com/>.
- [18] Edwards TL, Xue K, and Meenink HCM. "First-in-human study of the safety and viability of intraocular robotic surgery." In: *Nat Biomed Eng.* 2 (2018), pp. 649–656. doi: 10.1038/s41551-018-0248-4.
- [19] W.H.O.(WHO). *WHO launches first World report on vision*. 2019. URL: <https://apps.who.int/iris/rest/bitstreams/1257940/retrieve>.
- [20] W. Wei et al. "Enabling technology for microvascular stenting in ophthalmic surgery." In: *Journal of Medical Devices* 4 (2010).
- [21] P. Xu, Y. Jingjun, and B. S. Z. Guanghua. "Enumeration and Type Synthesis of One-DOF Remote-Center-of-Motion Mechanisms." In: *12th IFToMM World Congress* (2007), pp. 1–6.